ELECTRONIC SUPPORTING INFORMATION (ESI) FOR THE PAPER

A Structural and ^{1}H NMR Relaxometric Study on Novel Layered Carboxyalkylaminophosphonate Nanocrystals with Gd(III) Ions Located into the Framework.

Authors: *Antonio Scafuri, Marco Taddei, Riccardo Vivani, Fabio Carniato, Lorenzo Tei, Mauro Botta* and Ferdinando Costantino**

Analytical methods

- *Elemental Analysis.* The gadolinium and phosphorus contents were obtained by inductively coupled plasma optical emission spectroscopy using a Varian Liberty Series II instrument working in axial geometry, after mineralization of the sample with hydrofluoric acid. The carbon, hydrogen, and nitrogen contents were obtained with an EA 1108 CHN Fisons instrument.

- *Powder X-Ray Diffraction.* The PXRD patterns were collected in the 3-90 2θ range and with a 150 s/step counting time with the CuKα radiation on a PANalytical X'PERT PRO diffractometer, PW3050 goniometer, equipped with an X'Celerator detector. The long fine focus (LFF) ceramic tube operated at 40kV and 40mA.

- *Thermogravimetric Analysis.* TGA was performed using a Netzsch STA490C thermoanalyser under a 20 mL min^{-1} air flux with a heating rate of 5 °C min^{-1}.

Field Emission Scanning Electron Microscopy. FE-SEM images were collected with a LEO 1525-ZEISS instrument, working with an acceleration voltage of 15 kV.

- *Trasmission Electron Microcopy (TEM).* TEM images were collected with Philips 208 Transmission Electron Microscope working at 200 kV.

- *Relaxometric analysis.* The proton $1/T_1$ NMRD profiles were measured using a fast-field-cycling Stelar SmarTracer relaxometer at magnetic field strengths between 0.00024 and 0.25 T (which correspond to 0.01–10 MHz proton Larmor frequencies). The relaxometer was operated under computer control with an absolute uncertainty in $1/T_1$ of ±1%. Additional data points in the range of 20–70 MHz were obtained using a Stelar Relaxometer and a Bruker WP80 NMR electromagnet adapted to variable-field measurements (20–70 MHz proton Larmor frequency). The standard inversion–recovery method was employed (16 experiments, 2 scans) with a typical 90° pulse width of 3.5 μs, and the reproducibility of the T_1 data was ± 0.5%. The temperature was controlled using a Stelar VTC-91 variable temperature unit equipped with a copper-constantan thermocouple (uncertainty of ± 0.1 °C).

Synthetic procedures

Synthesis of the phosphonic ligands: The phoshonic acids were prepared according to a well-established Moedrizer-Irani phosphonomethylation process (Moedritzer, K.; Irani, R. R. J. Org. Chem. 1966, 31, 1603−1607), starting with α-amino-acid; the phosphonoalkylation of acidic amino protons placed next to a carboxyl functional group is conducted by using phosphorous acid and paraformaldehyde, so as to obtain the respective phosphono-amino-carboxylate acids.

N-phosphonometyl-glycine [$(H_2O_3PCH_2)NHCH_2CO_2H$] (H_4L^1) was purchased by Sigma-Aldrich.
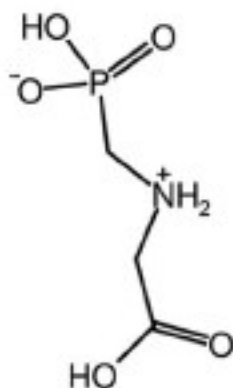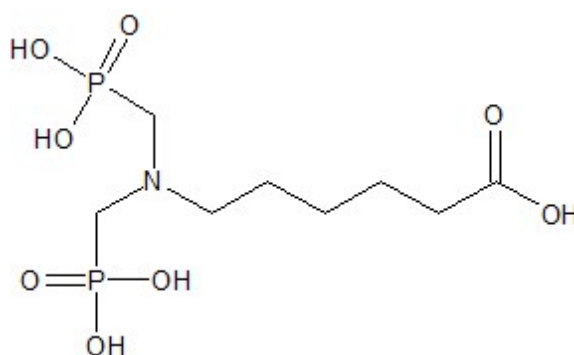

Figure 1: Molecular structure of glyphosate

Synthesis of N,N-bis-phophonomethyl-butanoic acid [$(H_2PO_3CH_2)_2N(CH_2)_3(CO_2H)$] ($H_5L^2$): 67 mmol (7 g) of 4-amino-butanoic acid $NH_2(CH_2)_3CO_2H$ and 138 mmol (11 g) of phosphorous acid were dissolved in a solution of 25 ml of H_2O and 25 mL of HCl 37%. The mixture was refluxed and 226 mmol (8 g) of paraformaldehyde were added slowly for 2 hours. At the end of addition, the mixture is maintained at reflux for one hour. The resulting solution was evaporated to dryness, affording an amber oil. The oil was purified with 2-propanol and washed over-night; a white solid was recovered by filtration under vacuum and dried in oven at 100 °C.
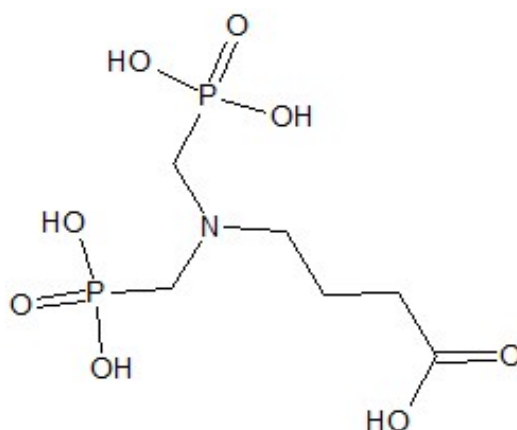
Figure 2: Molecular structure of diphosphonic-GABA derivate

***Synthesis of N,N-bis-phophonomethyl-caproic acid [(H₂PO₃CH₂)₂N(CH₂)₅(CO₂H)] (H₅L³):***

67 mmol (8.7 g) of 6-amino-caproic acid $NH_2(CH_2)_5CO_2H$ and 138 mmol (11 g) of phosphorous acid were dissolved in a solution of 25 mL of H_2O and 25 ml of HCl 37%. The mixture was refluxed and 226 mmol (8 g) of paraformaldehyde were added slowly for 2 hours. At the end of addition, the mixture is maintained at reflux for one hour. The resulting solution was evaporated to dryness, affording an amber oil. The oil was purified with 2-propanol and washed over-night; a white solid was recovered by filtration under vacuum and dried in oven at 100 °C.

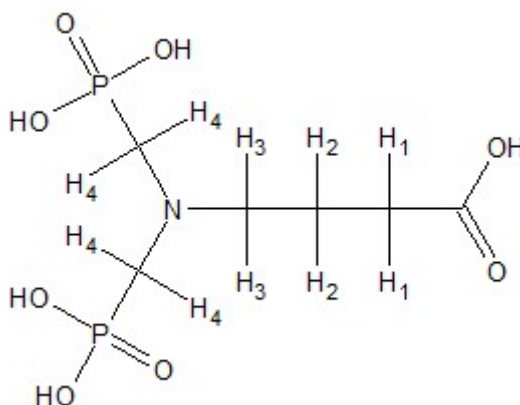*Figure 3: Molecular structure of diphosphonic-caproic derivate*

Structural Identification:

N-phosphonometyl-glycine: ^{1}H (D$_2$O, 400 MHz): δ 3.51 (alkyl-H$_1$, 2H, s), 3.69 (alkyl-H$_2$, 2H, s)
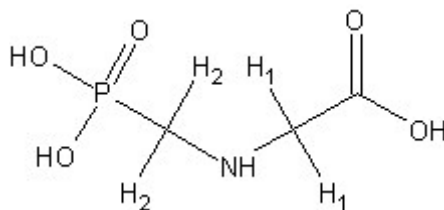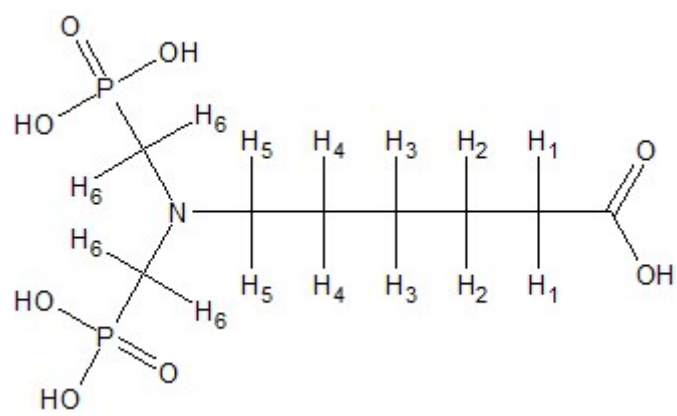
Figure 4: Molecular structure of glyphosate

N,N-bis-phophonomethyl-butanoic acid: ^{1}H (D$_2$O, 400 MHz): δ 3.45 (alkyl-H$_4$, 4H, s), δ 2.41 (alchyl-H$_3$, 2H, t, J = 0.16), 1.97 (alchyl-H$_1$, 2H, t, J = 0.4), 1.30 (alkyl-H$_2$, 2H, m).

Figure 5: Molecular structure of N,N-bis-phophonomethyl-butanoic acid

N,N-bis-phophonomethyl-caproic acid: ^{1}H (D$_2$O, 400 MHz): δ 3.43 (alkyl-H$_6$, 4H, s), 2.31 (alkyl-H$_5$, 2H, t, J = 0.39), 2.12 (alchyl-H$_1$, 2H, t, J = 0.19), 1.65 (alkyl-H$_2$, 2H, m), 1.57 (alkyl-H$_3$, 2H, m), 1.32 (alkyl-H$_4$, 2H, m).

Figure 6: Molecular structure of diphosphonic-caproic derivate

Synthesis of Gd phosphonates

The compounds were synthesized under mild hydrothermal conditions:

Synthesis of Gd[(HPO$_3$CH$_2$)NHCH$_2$(CO$_2$)(HPO$_3$CH$_2$)NHCH$_2$(CO$_2$H)] (1)

1 mmol of [(H$_2$O$_3$PCH$_2$)NHCH$_2$(CO$_2$H)] N-phosphono-methylglycine was solubilized in 2 mL of distilled water; to dissolve the phosphonic acid, 1 ml of NaOH 1 M was added dropwise under stirring. Meantime, a solution of 0.5 mmol of Gd(NO$_3$)·6H$_2$O in 2 mL of distilled water was prepared. The used P/Gd ratio is 2. The two solutions were reunited together in a closed Teflon bottle and heated at 80°C for 16 hours. The white solid was recovered by filtration under vacuum, washed with deionized H$_2$O and dried in oven at 100°C; white microcrystals were collected. Analysis Calcd for C$_6$H$_{13}$N$_2$O$_{10}$P$_2$Gd (1): Gd 32.28% (obs 31.3%), P: 12.8% (obs 12.0%)

Synthesis of Gd[(HPO$_3$CH$_2$)(PO$_3$CH$_2$)N(CH$_2$)$_3$(CO$_2$H)]·(H$_2$O) (2)

1 mmol of [(H$_2$PO$_3$CH$_2$)NH(CH$_2$)$_3$(CO$_2$H)] N,N-bis-phosphonomethyl-butanoic acid was solubilized in 2 mL of distilled water; to dissolve the diphosphonic acid, 1 ml of NaOH 1 M was added dropwise under stirring. Meantime, a solution of 0.5 mmol of Gd(NO$_3$)·6H$_2$O in 2 mL of distilled water was prepared. The ratio P/Gd is 4. The two solutions were reunited together in a closed Teflon bottle and heated at 80°C for 3 days. The white solid was recovered by filtration under vacuum, washed with deionized H$_2$O and dried in oven at 100°C; white microcrystals were collected. Analysis Calcd for C$_6$GdNO$_9$P$_2$H$_{12}$ (2): Gd 33.3% (obs. 32.9%), P 12.9% (obs. 12.1%)

Synthesis of Gd[(HPO$_3$CH$_2$)(PO$_3$CH$_2$)N(CH$_2$)$_5$(CO$_2$H)]·(H$_2$O) (3)

0.5 mmol of [(H$_2$PO$_3$CH$_2$)$_2$NH(CH$_2$)$_5$(CO$_2$H)] N,N-bis-phophonomtehyl-caproic acid was solubilized in 10 mL of distilled water; to dissolve the diphosphonic acid, 0.06 ml of NH$_3$ 3% solution (1 mmol) was added dropwise under stirring. Meantime, a solution of 0.5 mmol of Gd(NO$_3$)·6H$_2$O in 10 mL of distilled water was prepared. The used P/Gd ratio is 2. The two solutions were reunited together in a closed Teflon bottle, and was added inside few drops of HNO$_3$ 65%. Finally, the dispersion was heated at 80°C for 3 days. The white solid was recovered by filtration under vacuum, washed with deionized H$_2$O and dried in oven at 100°C; white microcrystals were collected. Analysis Calcd for C$_8$GdNO$_9$P$_2$H$_{16}$ (3): Gd 31.5% (obs 30.3%) P 12.4% (obs 11.9%)

# Structure determination and refinement from X-Ray Powder data for 1 and 3

Indexing of the diffraction patterns of **1** and **3** was performed using the *TREOR* program. The analysis of systematic extinctions for space group assignment was performed using the *Chekcell* program. The structural model was determined using the real space global optimization methods implemented in the *FOX* program by using the parallel tempering algorithm. An isolated Gd ion and the molecular structure of the three ligands, with restrained bond lengths and angles, was imported as z-matrix and the optimization was carried out until three suitable model were found. Rietveld refinement of the found structural models was performed using the *GSAS* program.

First, zero-shift, unit cell, background, and profile-shape parameters were refined. A corrected pseudo-Voigt profile function (six terms) with two terms for the correction of asymmetry at the low-angle region was used. Then, atomic coordinates were refined by restraining the bond distances to the following values: Gd-O = 2.5(5) Å, P-O = 1.56(5) Å, P-C = 1.83(5) Å, aliphatic C-C = 1.54(5) Å, C-N = 1.32(5), C-O carboxylic 1.23(5) Å. The statistical weight of these restraints was decreased as the refinement proceeded. At the end of the refinement the shifts in all parameters were less than their standard deviations.
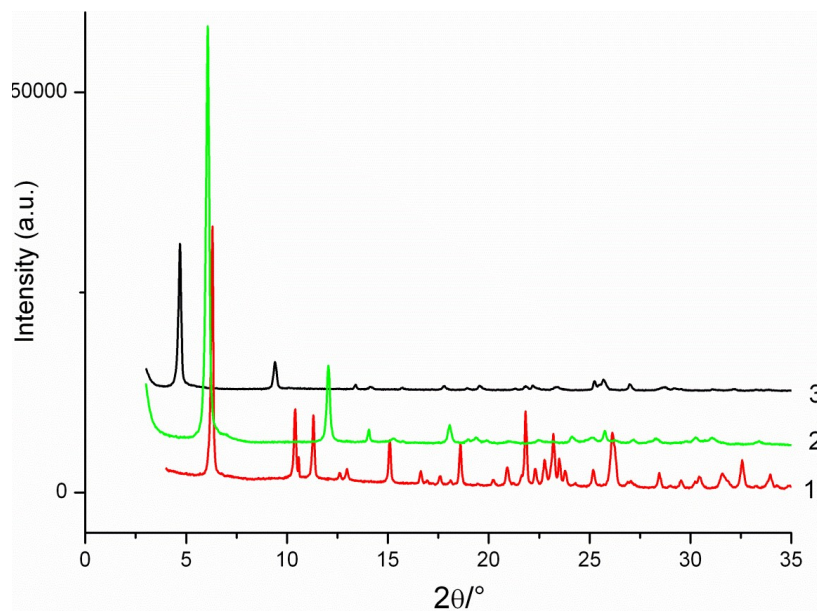
Figures and Tables
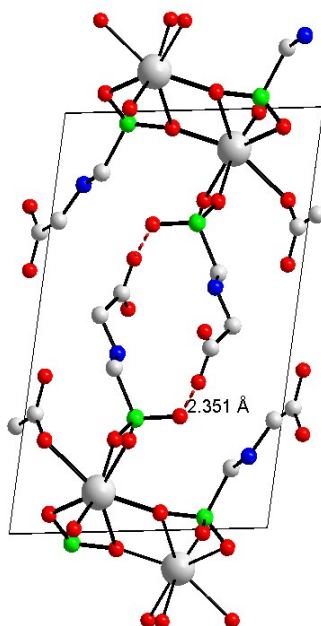
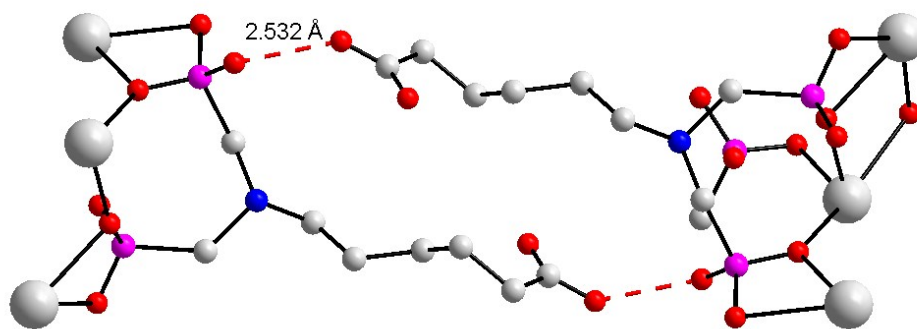**Figure 1S.** H- bonds interactions between carboxylic and phosphonic groups in **1**.
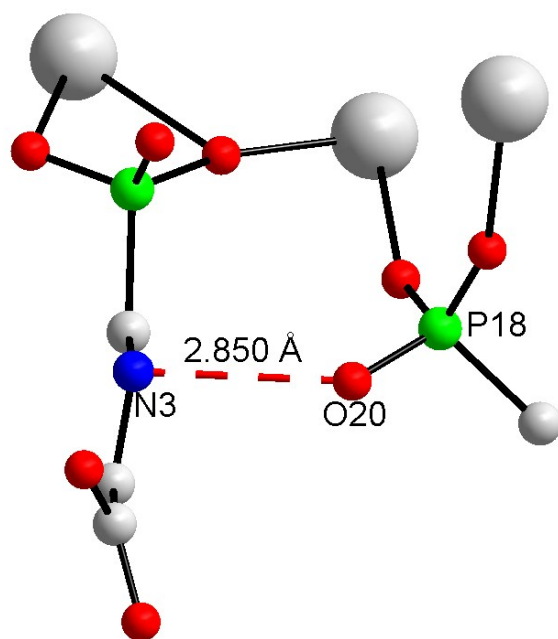
Figure 2S. Interactions between protonated N-atoms and phosphonic oxygen atoms in **1.**
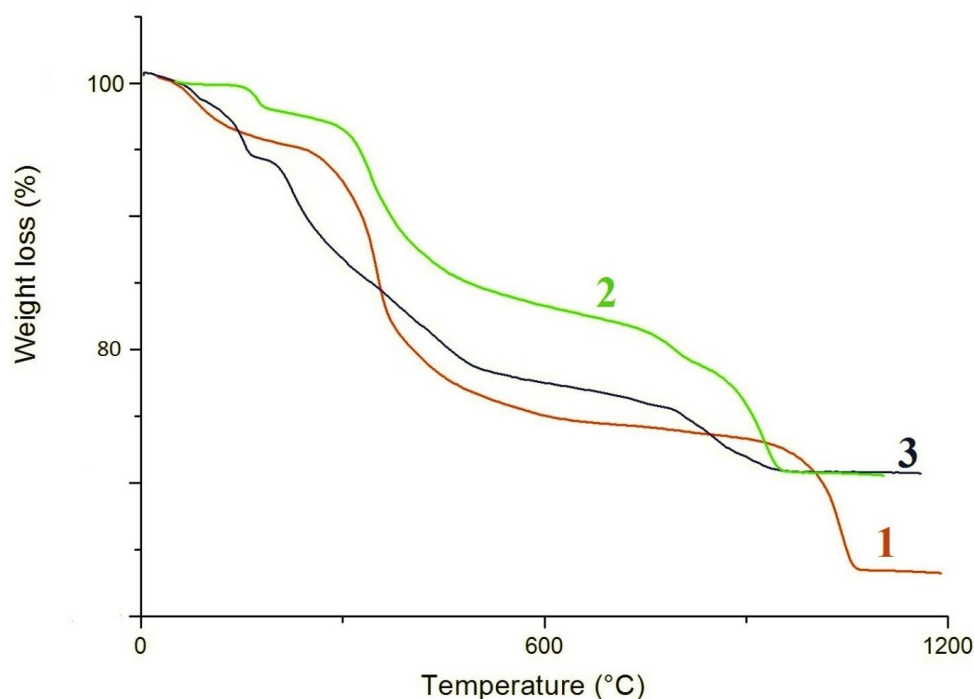


Figure 3S. XRPD patterns of **1**, **2** and **3.**

**Figure 4S.** H-bonds interactions between carboxylic and phosphonic groups in **3.**

Figure 5S. TG curves of **1**, **2** and **3** samples.TG curves for compounds **1** and **2** showed remarkable thermal stabilities up to about 300 °C, while, for compound **3**, decomposition of organic moiety already occur at lower temperatures; above this temperature, a gradual weight loss up to about 800 °C was observed. In compounds **2** and **3**, an initial weight loss of about 2% of the total weight was observed over the temperature range 100–120 °C, which corresponded to the loss of coordination H$_2$O bonded to gadolinium, that has been found during the structural refinement; this weight loss is

absent in compound **1**, as confirmed by X-ray crystallography. The second weight loss is divided in two step: the first one, over the 205-600 °C temperature range, is due to combustion of amino-carboxylate chains, whereas the second step, over the 600-1000 °C temperature range, is due to condensation of phosphate groups. For all compounds, a gradual weight loss was observed up to 900°C, thereby suggesting that combustion of organic groups occurred-. In all cases, at the end of analysis, an equimolar mixture of $Gd(PO_3)_3$ and $GdPO_4$ was found, that was compatible with total weight loss (35% for compound **1**; 40% for compounds **2** and **3**).
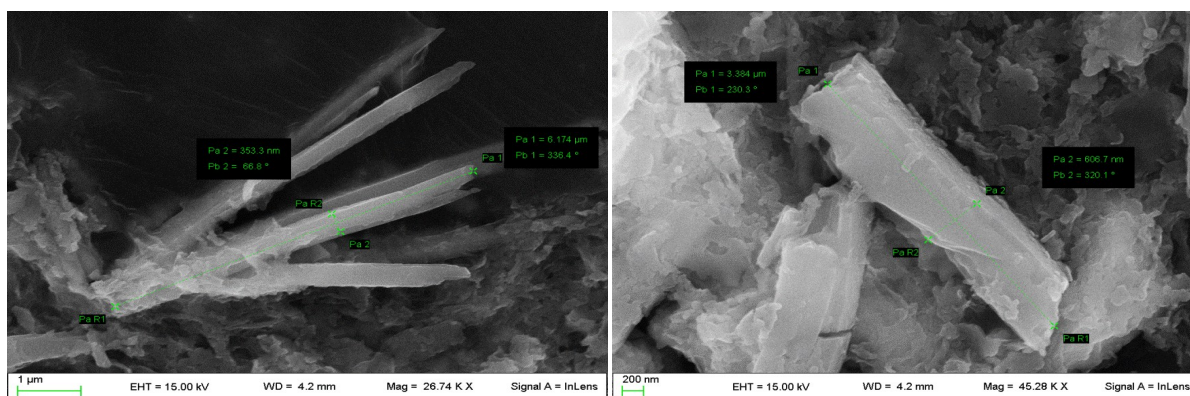
Figure 6S. SEM images of crystal aggregates of **1.** Hydrothermal synthesis leads to the formation of microcrystalline aggregates which are in dimensional order of approximately 6-7 microns.
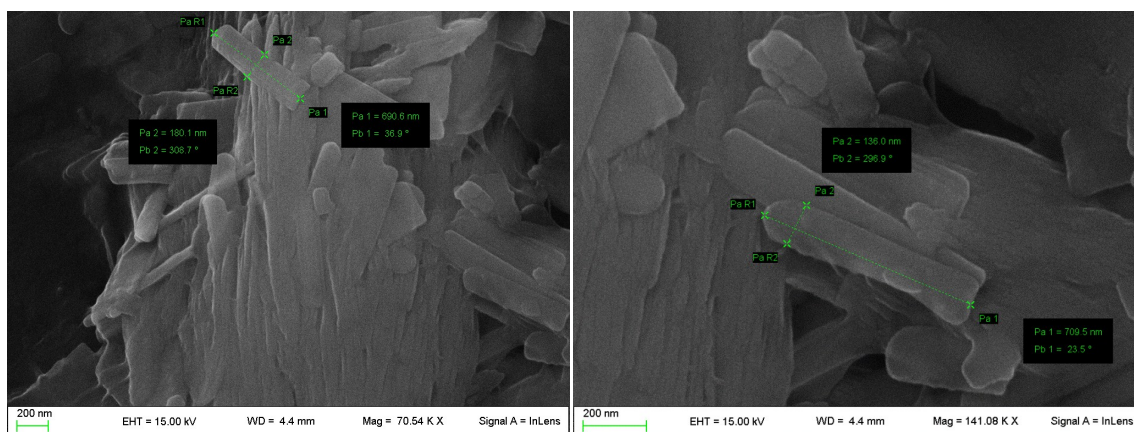

**Figure 7S.** SEM images of crystal aggregates of **2.**
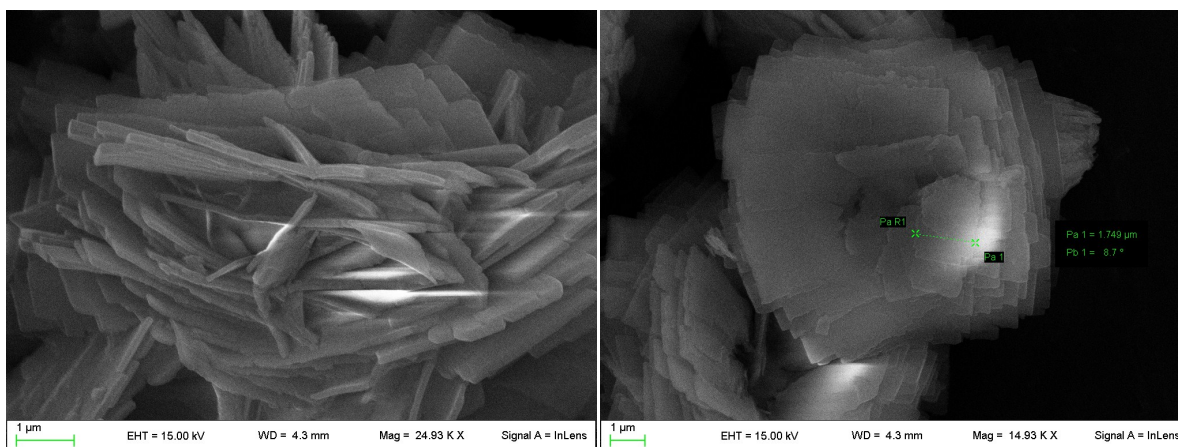
**Figure 8S.** SEM images of crystal aggregates of **3.**

Figure 9S. The Tyndall effect of aqueous dispersion of sample **1.** Stable and homogeneous dispersions of these compounds were obtained by stirring the sample in a deionized water solution, that contained a small amount (4/5 drops) of propilamine 0.2 M, and then ultrasonicated for 10 minutes; Tyndall Effect was established on compound **1**; all other two compounds showed similar behavior.
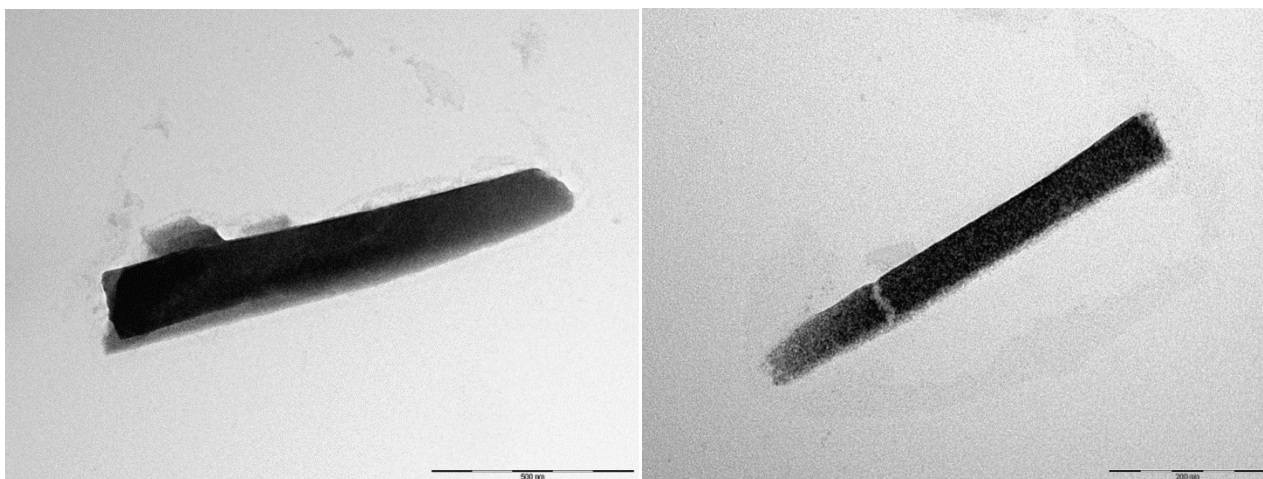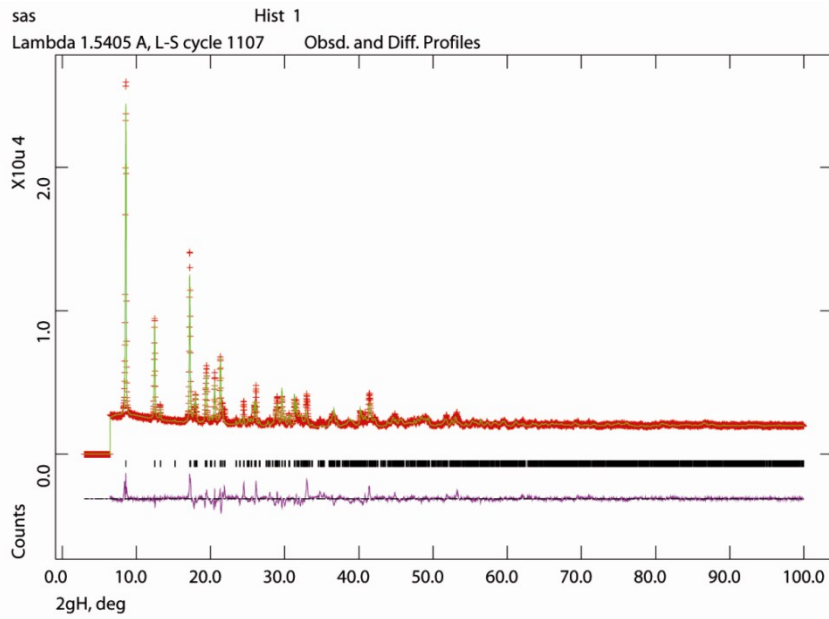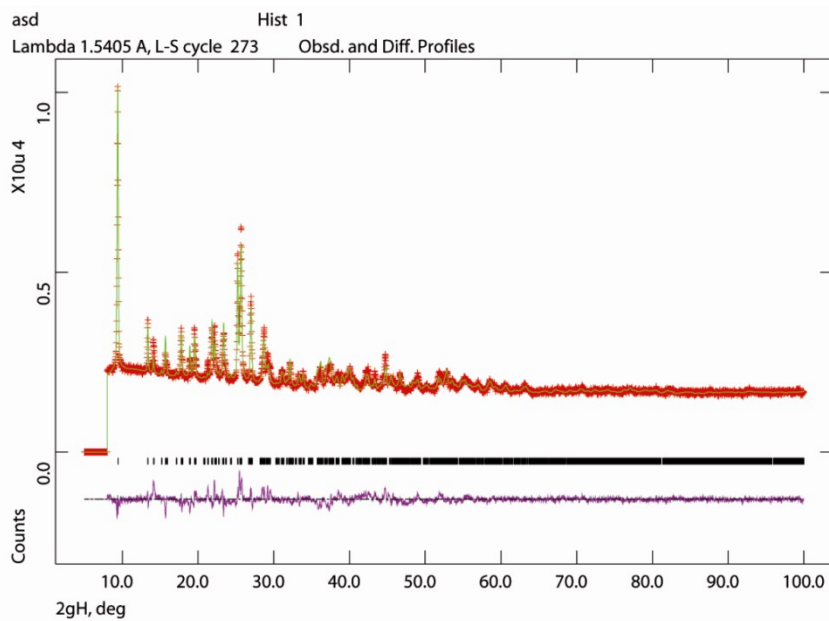
Figure 10S. TEM images of crystals of **1.**
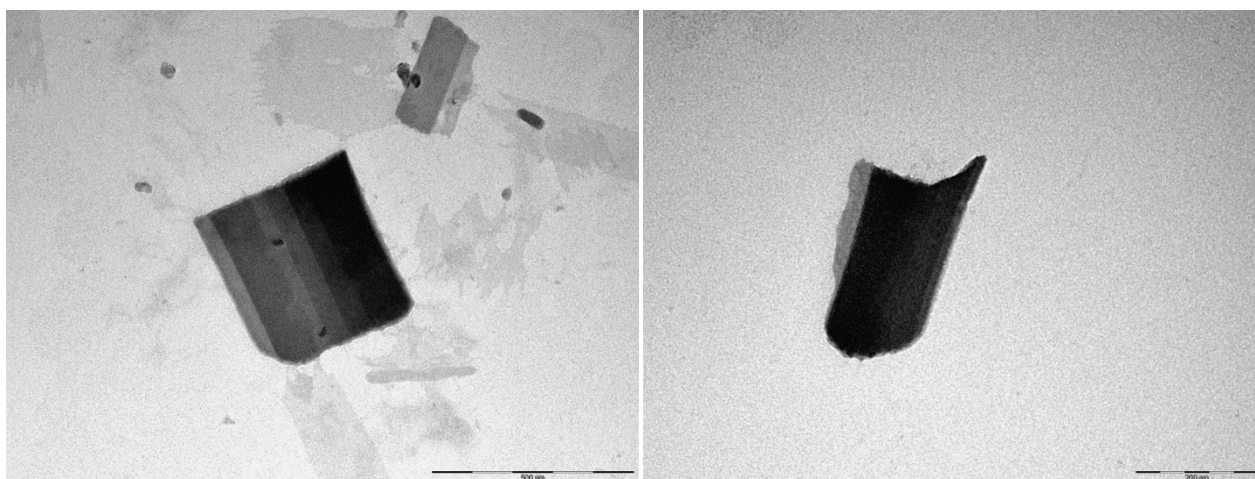
Figure 11S. TEM images of crystals of **2.**
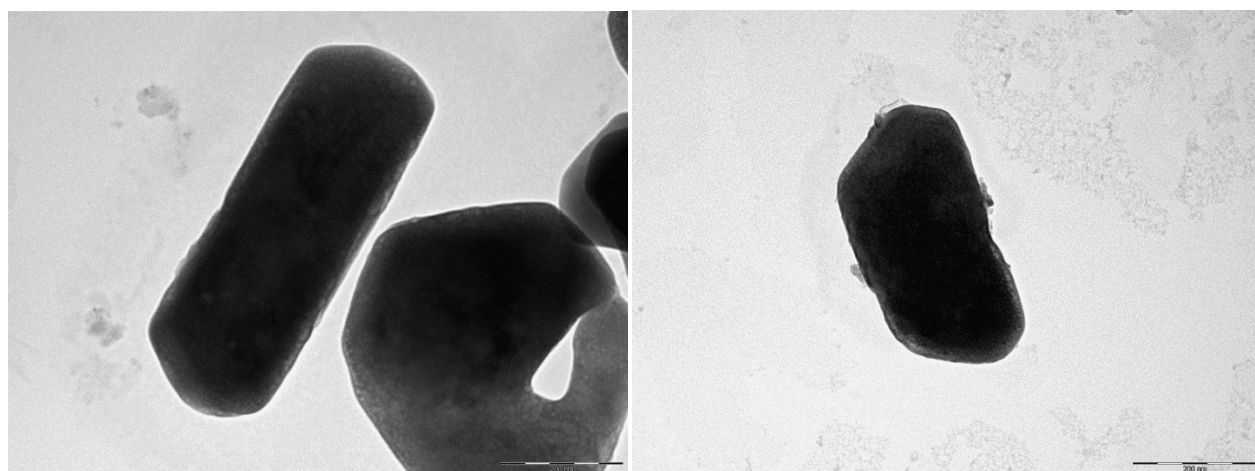
Figure 12S. TEM images of crystals of **3.**

Figure 13S. Rietveld plot for **1.**

**Figure 14S.** Rietveld plot for **3.**

Table 1S. Crystallographic and refinement details for **1** and **3**

| Compound	1	3
Empirical formula	$C_6 Gd N_2 O_{10} P_2 H_6$	$C_8 Gd N O_9 P_2 H_{15}$
Formula weight	484.27	499.28
Crystal system	Triclinic	Monoclinic
Space Group	*P -1*	*P21/c*
a/ Å	5.5418(3)	18.783(4)
b/Å	8.8674(4)	7.0572(6)
c/Å	14.270(1)	10.335
α/deg.	97.146(4)	
β/deg.	96.016(4)	90.38(1)
γ/deg.	103.956(4)	
Volume/Å^3	668.61(6)	1370.0(4)
Z	2	4
T/°C	25	25
Calculated density/g·cm^{-3}	2.81	2.29
Data range/ $2q$ ·deg^{-1}	3 - 100	3 - 100
Wavelength/Å	1.54056	1.54056
N. of data points	5705	5409
Reflections collected	1157	3015
N. of parameters	92	84
N. of restraints	51	60
R_p	0.0458	0.0298
R_{wp}	0.0619	0.0415
$R_F 2$	0.066	0.132
GOF	1.22	2.28

Table 2S. Selected best-fit parameters obtained from the analysis of the $1/T_1$ NMRD profiles (298 K) of **1**, **2** and **3** samples.[a]

	Δ^2 (10^{19} s^{-2})	τ_V (ps)	^{SS}q	^{SS}r (Å)	$^{SS}\tau_R$ (ps)
1	4.3	33	1	3.5	275
2	4.0	29	0.3	3.5	240
3	4.1	34	/	/	/

[a]For the outer sphere (OS), parameters a (distance of closest approach) and ^{298}D (relative diffusion coefficient for solute and solvent), the values of 9.7 Å and 2.24 x 10^{-5} cm^2 s^{-1} were used. ^{SS}r parameter was fixed during the fitting.
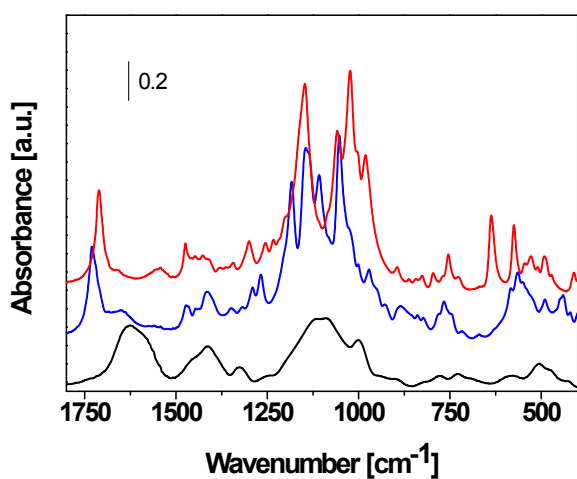
Figure 15S. FT-IR spectra of **1** (black curve), **2** (blue) and **3** (red) samples in the 1800-400 cm^{-1} range.
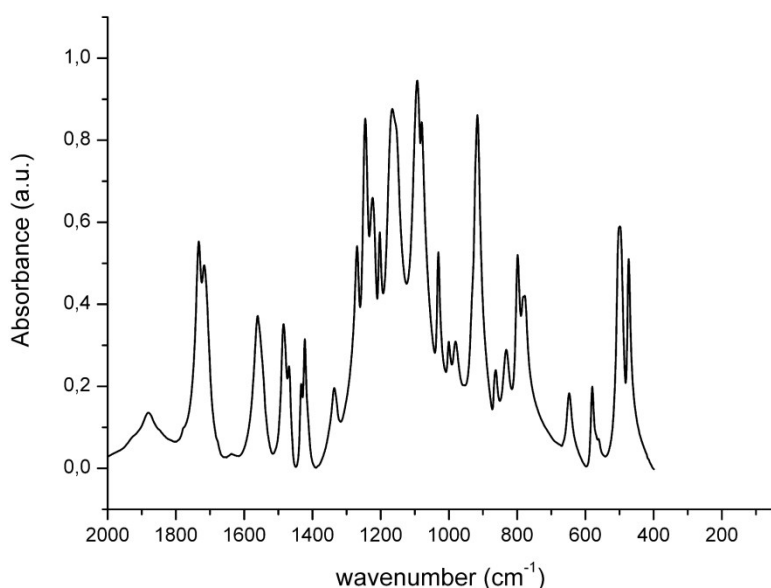
Figure 16S. FT-IR spectrum of the ligand **H₄L¹**

IR spectra of **1, 2** and **3** samples have been reported in the Fig. 15S. Prior to the analysis, all the materials were dispersed in dehydrated KBr matrix (10 wt%).

Specific attention was addressed to the low wavenumbers region, from 1800 to 900 cm⁻¹, where the bands typical of carboxylic/carboxylate and phosphonate groups fall. Interestingly, the spectrum of sample **1** shows an intense peak at 1610 cm⁻¹ which can be ascribed to the asymmetric stretching mode of the COO⁻ groups. This absorption falls at lower frequencies if compared to the band at *ca.* 1720 cm⁻¹ of samples **2** and **3**. This down frequency shift in the absorption is a clear indication that the carboxylate groups in the sample **1** are involved in the coordination of Gd^{3+} metal centers. For samples **2** and **3**, this signal at 1610 cm⁻¹ was not present, indicating that the carboxylic groups do not coordinate the Gd^{3+} ions.

For comparison the FT-IR spectrum of pure **H₄L¹** is also reported in figure 16S. The asymmetric stretching of carboxylate falls at 1732 cm⁻¹, which is typical of uncoordinated carboxylic groups.

Moreover, further differences between sample **1** and samples **2** and **3** can be observed in the frequencies range typical of phosphonate groups (1200-900 cm⁻¹). The correct attribution of the all peaks ascribed to the asymmetric and symmetric stretching of the P-O groups is very complicated and usually this spectral range is just qualitatively analyzed (A. Donnadio, M. Nocchetti, F. Costantino, M. Taddei, M. Casciola, F. da Silva Lisboa, R. Vivani, *Inorg. Chem.* 2014, 53, 13220−13226). Nevertheless, as a general comment, both the samples **2** and **3** show comparable absorptions. These peaks, that appear well resolved, may be indicative of a homogenous environment experimented by the P-O units. In opposite, the spectrum of sample **1** shows a broadened band in the 1200-1000 cm⁻¹ range, thus suggesting a more heterogeneous arrangement of the phosphonate groups.